

Wideband and Continuously Tunable Microwave Photonic Phase Shifter Based on an Active InP/InGaAsP Microring Resonator

Jian Tang,^{1,2,3} Ming Li,^{2,3} Robert S. Guzzon,⁴ Larry A. Coldren,⁴ and Jianping Yao^{1,*}

1. Microwave Photonics Research Laboratory

School of Electrical Engineering and Computer Science, University of Ottawa
Ottawa, Ontario K1N 6N5, Canada

2. State Key Laboratory on Integrated Optoelectronics,
Institute of Semiconductors, Chinese Academy of Sciences
Beijing 100083, China

3. School of Electronics, Electrical and Communication Engineering
University of Chinese Academy of Sciences, Beijing 100049, China

4. Department of Electrical and Computer Engineering
University of California Santa Barbara
Santa Barbara, California 93116, USA

*Corresponding author: jpyao@uottawa.ca

Abstract—We propose and experimentally demonstrate a wideband and continuously tunable microwave photonic (MWP) phase shifter based on an active InP/InGaAsP microring resonator (MRR) incorporating two semiconductor optical amplifiers (SOAs) and a phase modulator (PM). By tuning the gain provided by the SOAs, the loss in the ring cavity can be compensated and the extinction ratio of a resonance is decreased to nearly 0 dB, while maintaining the optical phase shift range of nearly 2π within the resonance bandwidth. A theoretical analysis is performed. The key advantages of using the proposed MRR to achieve a microwave phase shifter are that the power variation at the output of the phase shifter is minimized during phase tuning and the microwave phase can be continuously tuned by tuning the PM in the MRR theoretically. The proposed phase shifter is experimentally demonstrated. A continuously tunable microwave phase shift over a phase tuning range of 291° from 5 GHz to 20 GHz by tuning the injection current to the PM is implemented. The microwave power variation is lower than 5 dB.

Keywords—integrated optics devices, ring resonators, phase shift.

I. INTRODUCTION

Microwave phase shifter is one of the most important devices that is widely used in modern microwave systems, such as Radar [1], wireless communications [2], 5G networks [3], and warfare systems [4]. Pure electronic microwave phase shifters are limited by the bandwidth and tunability which may not be able to meet the requirements needed by modern microwave systems [4-6]. Modern photonics, especially integrated photonics, with key features such as broad bandwidth, large tunability and small size can be employed to implement microwave photonic (MWP) phase shifters [6-9]. The most representative integrated device employed to implement an MWP phase shifter is a micro-ring resonator (MRR) [10-12]. By locating the optical carrier in the bandwidth of a resonance, a phase shift is introduced to the optical carrier. Then, by beating the optical carrier with a sideband, a phase shifted microwave signal with its phase shift translated from the optical carrier is generated. By cascading two MRRs on a silicon on insulator (SOI) platform, a maximum microwave phase shift range of 600° was achieved at a

microwave frequency of 40 GHz [13]. A high Q MRR based on aluminum nitride (AlN) material system was used to realize an MWP phase shifter. A phase shift range of 332° over a frequency range from 4 GHz to 25 GHz was demonstrated [14]. A cascaded MRRs based on silicon nitride (Si_3N_4) material system was also employed to demonstrate an MWP phase shifter with a 2π phase tunable range [15]. An MRR based on InP/InGaAsP material system has the key advantage of electrical pumped optical gain, which does not exist in the above-mentioned material systems, and thus has the ability to provide a loop gain to compensate for the loss. It makes an InP/InGaAsP-based MRR has an additional degree of flexibility to control its spectral response, thus making it more suitable for realizing an MWP phase shifter.

In this letter, we propose and experimentally demonstrate an add-drop type InP/InGaAsP material based MRR which is employed to realize a continuously tunable microwave phase shifter. Two semiconductor optical amplifiers (SOAs) and a phase modulator (PM) are integrated in the ring cavity to provide an optical gain and realize phase shift tuning, respectively. When the loss in the active MRR is compensated by the gain provided by the SOAs, the optical extinction ratio of a resonance is reduced to nearly 0 dB, while a large phase shift range in a resonance bandwidth is maintained almost unchanged. The problem that a large phase shift may result in a large microwave power variation for an MRR-based MWP phase shifter is solved. The key advantages of using the proposed active MRR to achieve an MWP phase shifter are that the power variation at the output of the phase shifter is minimized during phase tuning and the microwave phase can be continuously tuned by tuning the PM in the MRR theoretically. The proposed MRR-based MWP phase shifter is demonstrated experimentally. A continuously tunable microwave phase shift over a phase tuning range of 291° from 5 GHz to 20 GHz by tuning the injection current to the PM is implemented. The microwave power variation is lower than 5 dB.

II. PRINCIPLE

Figure 1 (a) shows the schematic of the proposed add-drop type InP/InGaAsP-based MRR. As can be seen the MRR has two SOAs (SOAs1-2) and a PM (PM0) in the cavity. Two tunable couplers (TCs) consist of two PMs (PM1 and PM2) and two multi-mode interferometer (MMI) 3-dB couplers. The

This work was supported by the Natural Sciences and Engineering Research Council of Canada (NSERC). Jian Tang was supported by the China Scholarship Council.

coupling ratio of each TC can be adjusted by tuning the injection currents to the PMs in a TC. By tuning the injection current to PM0 in the ring cavity, the resonance frequency of the MRR can be continuously tuned for tens GHz. In addition, four other SOAs (SOAs3-6) are integrated in the four straight waveguides which are mainly used to compensate for the coupling loss from the lens fiber to the chip. Note that the SOAs integrated on the chip can operate in two states. When an SOA is forward biased, it operates in the amplification states, while when an SOA is reverse biased, it operates as an optical absorber. Fig. 1 (b) shows the photograph of the proposed chip which is wire-bonded to a polychlorinated biphenyl carrier for the experimental measurement. Two lens fibers are used to couple the light into (or out from) the chip through the edge couplers integrated on the chip.

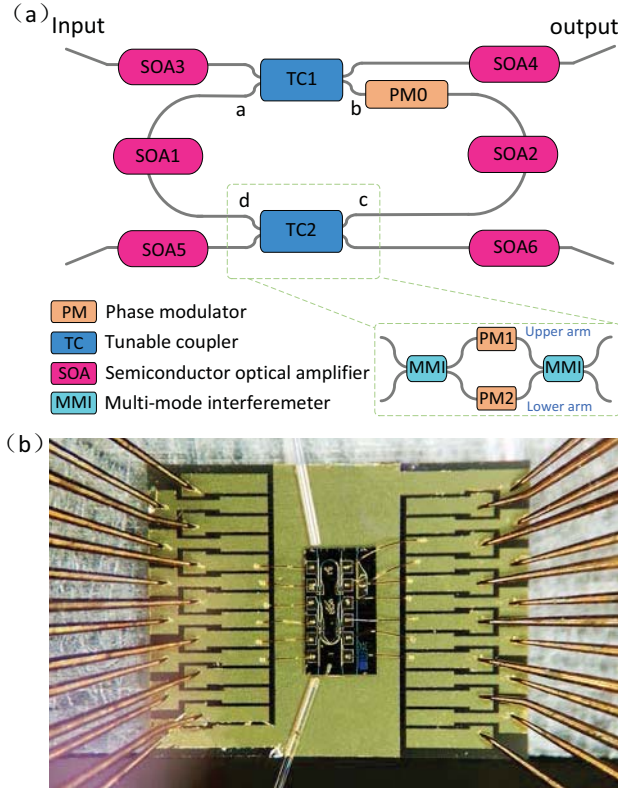


Fig. 1. (a) The schematic of the proposed active MRR. The inset shows the details of the tunable coupler. (b) The photograph of the proposed MRR chip.

To simplify the analysis, the self-coupling coefficients of the two TCs are regarded as constant over the frequency range and the coupling loss is ignored. By employing the transfer matrix method, the transfer function of the proposed add-drop type InP/InGaAsP-based MRR can be expressed as [16]

$$H(\omega) = \frac{t_{TC1} - t_{TC2}G_1G_2e^{-j\varphi(\omega)}}{1 - t_{TC1}t_{TC2}G_1G_2e^{-j\varphi(\omega)}} \quad (1)$$

where t_{TC1} and t_{TC2} are the self-coupling coefficients of TC1 and TC2, respectively. G_1 is the accumulated transmission gain from point d to point a and G_2 is the accumulated transmission gain from point b to point c. $\varphi(\omega) = \omega\tau$, ω is the angular frequency and τ is the one round trip time for the light transmitting in the ring circuit. The resonance frequency is given by $\omega\tau = 2n\pi$ (n is an integer). When PM0 in the ring circuit is tuned, τ is changed. Thus, the resonance frequency is changed. By tuning the gain

provided by SOA1 and SOA2, the loss in the ring resonator can be compensated. In this case, $t_{TC2}G_1G_2$ is close to unity. Then, Eq. (1) can be written as

$$T = \frac{t_{TC1} - e^{-j\varphi(\omega)}}{1 - t_{TC1}e^{-j\varphi(\omega)}} = -\frac{e^{-j\varphi(\omega)/2} - t_{TC1}e^{j\varphi(\omega)/2}}{e^{j\varphi(\omega)/2} - t_{TC1}e^{-j\varphi(\omega)/2}} \quad (2)$$

One can find that the expression in the numerator ($e^{-j\varphi(\omega)/2} - t_{TC1}e^{j\varphi(\omega)/2}$) is a complex conjugate of the expression in the denominator ($e^{j\varphi(\omega)/2} - t_{TC1}e^{-j\varphi(\omega)/2}$). Thus, the magnitude response (T) of the transmission is unity which can be written as

$$|T| = |H(\omega)|^2 = 1 \quad (3)$$

The phase response in transmission can be written as [11]

$$\phi(\omega) = \pi + 2 \tan^{-1} \left[\frac{(1 + t_{TC1}) \sin\left(\frac{1}{2}\varphi(\omega)\right)}{(1 - t_{TC1}) \cos\left(\frac{1}{2}\varphi(\omega)\right)} \right] \quad (4)$$

Thus, the phase shift range within the resonance maintains 2π theoretically when the $\varphi(\omega)$ increases from $(2n-1)\pi$ to $(2n+1)\pi$, n is an integer.

III. EXPERIMENTS

The proposed MRR is fabricated based on the InP/InGaAsP material system and the use of the MRR to achieve MWP phase shifter is experimentally evaluated. In the experiment, the self-coupling coefficient of TC1 is first measured. SOA3 is forward biased at an injection current of 20 mA to compensate for the coupling loss from the lens fiber to the chip. SOA4 is reverse biased with a voltage of -3 V to make it works as a photodetector (PD). By tuning the injection current from 0 mA to 7 mA which is applied to PM2 of TC1, the self-coupling coefficient is recorded, as shown in Fig. 2(a). The self-coupling coefficient of TC2 is measured in the same way, which is shown in Fig. 2(b). To obtain a small extinction ratio at the resonance bandwidth, the injection current applied to PM2 in TC2 is tuned to 2 mA to get a largest t_{TC2} .

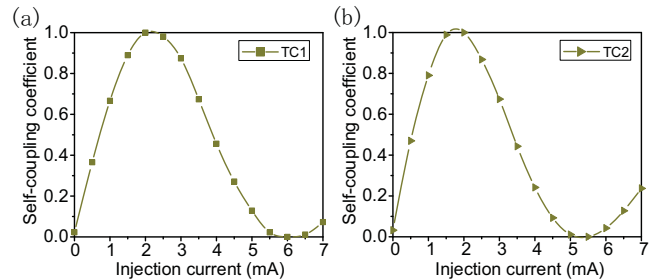


Fig. 2. Experimentally measured tunable self-coupling coefficients of TC1 and TC2.

Then, the transmission response of the MRR is characterized. The injection currents to SOA1 and SOA2 are set to 24 mA and 22 mA. The injection current to PM0 in the ring cavity is set to 0.8 mA. Both SOA3 and SOA4 are biased with a current of 20 mA to compensate for the coupling loss, and SOA5 and SOA6 are reverse biased to prevent from unexpected light reflection. We first use an optical vector network analyzer (OVNA, Luna 5400) to measure the

magnitude response, as shown in Fig. 3(a). As can be seen the free spectral response (FSR) of the MRR is around 0.203 nm (or 25.38GHz).

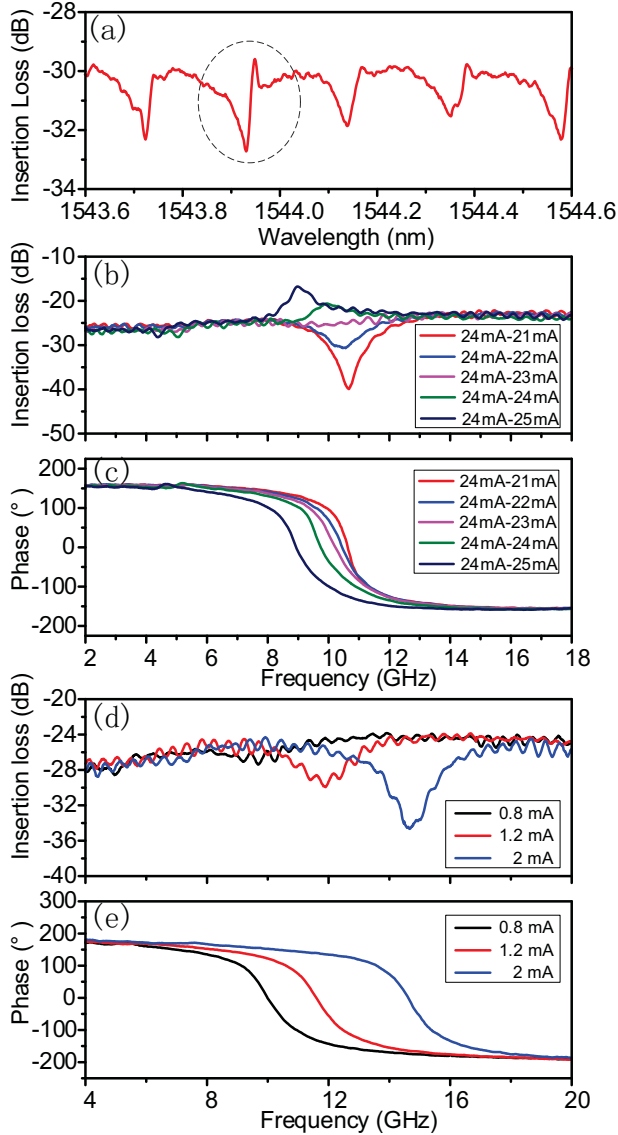


Fig. 3. The measurement results of the active MRR. (a) The magnitude response. (b) The magnitude response at 1543.92 nm and (c) the phase response. (d) The magnitude response when the resonance wavelength is tuned by PM0 and (e) the corresponding phase response.

Since the resolution of the OVNA is not high enough to measure the details of the spectral response of the MRR, we build a measurement system based on single sideband modulation to get a high resolution spectral response measurement through sweeping the sideband [17, 18]. The optical carrier is set at 1544.002 nm with the lower sideband sweeps from the optical carrier to a shorter wavelength. Here, the injection current to SOA1 is fixed at 24 mA. The extinction ratio at a resonance at 1543.92 nm is decreased when the injection current to SOA2 is increased from 20 mA to 23 mA, as shown in Fig. 3(b). When the injection current is larger than 23 mA, the gain will be greater than the loss in the ring cavity, but the lasing still does not start. Thus, the response of the MRR should be stable when the injection current applied on SOA2 is less than 23 mA. Fig. 3(c) shows the phase response when the injection current to SOA2 is increasing. As can be seen the phase shift range of about 300° is maintained almost unchanged. A slight resonance frequency

shift, as shown in Fig. 3(b) and (c), is mainly caused by the thermal effect introduced by the SOAs. Fig. 3(d) shows the resonance wavelength tuning of the MRR. As can be seen the resonance frequency is shifted from 9.7 GHz to 14.7 GHz when the injection current applied to PM0 is increased from 0.8 mA to 2 mA. During the wavelength tuning, the phase response is laterally shifted, but the phase shift range is remained almost unchanged (shown in Fig. 3(e)).

The MRR is then employed to implement an MWP phase shifter. The experimental setup is shown in Fig. 4. An optical carrier from a tunable laser source (TLS, Anritsu MG9638A) is modulated by a microwave signal generated by a vector network analyzer (VNA, Agilent E8364A) at a PM. After amplification by an erbium-doped fiber amplifiers (EDFA), the optical signal is sent to a tunable bandpass optical filter (OF) where one sideband is filtered out, to get an optical single-sideband (OSSB) signal. Then, the OSSB signal is coupled into the MRR through a polarization controller (PC2). The optical signal at the output of the MRR is detected by a PD to recover the microwave signal, which is sent to the VNA for intensity and phase analysis.

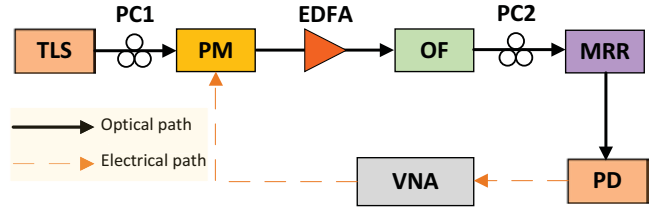


Fig. 4. Experimental setup for the proposed MWP phase shifter.

In the experiment, the wavelength of the optical carrier is set at 1543.884 nm, located at the resonance wavelength shown in Fig. 3(d) when the injection current to PM0 is 1.2 mA. The two sidebands are located at outside of the resonance, and one sideband is removed by the optical filter. To avoid the nonlinear effect in the MRR, the power of the optical carrier light is controlled less than -3 dBm before coupling into the MRR. A phase shift is introduced to the optical carrier from the phase response of the MRR, and the phase shift can be tuned by tuning the injection current to PM0. The beating between the optical carrier and the sideband will translate the phase shift in the optical carrier to the microwave signal.

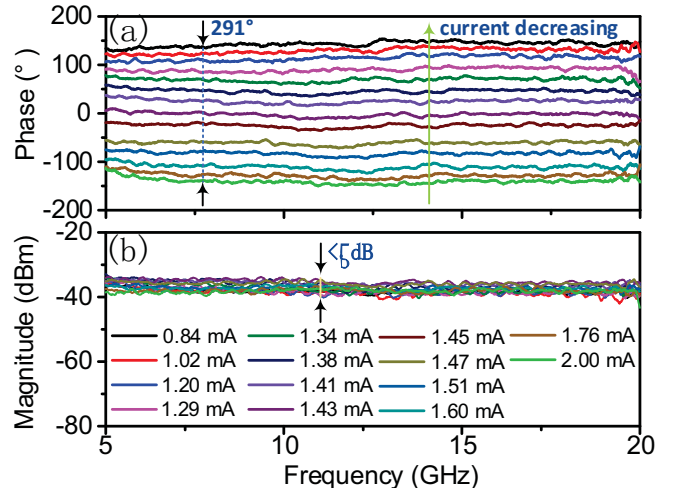


Fig. 5. Experimental results of the (a) phase response and (b) magnitude response of the phase shifter by decreasing the injection current applied on the PM in the ring cavity.

In the experiment, the injection currents to SOA3 and SOA4 are 20 mA. SOA5 and SOA6 are reverse biased with an identical voltage of -3 V. The injection current to SOA1 is set at 24 mA and the injection current to SOA2 is set at 23 mA. The injection currents applied to TC1 and TC2 are 1.5 mA and 2 mA, respectively. By tuning the injection current to PM0 from 2 mA to 0.84 mA, a phase shift from -148° to 143° with a total phase tunable range of 291° for a microwave frequency range from 5 GHz to 20 GHz is realized, as shown in Fig. 5(a). The microwave power variation is controlled small by fixing the injection currents which are applied to SOA1 and SOA2 to make the gain compensate the loss in the resonance cavity. As can be seen, in Fig. 5(b), the microwave power variation is smaller than 5 dB. This power variation can be attributed to the noise of the SOA and thermal noise in the chip. Once the chip is well temperature controlled, the microwave power variation during phase shifting can be suppressed. Moreover, since the MRR used in our experiment is an active device without packaging, the microwave power variation due to environmental changes is relatively high, which can be reduced if the device is well packaged. The bandwidth of the proposed MWP phase shifter is mainly limited by the FSR of the MRR. By reducing the length of the ring cavity, the FSR of the MRR could be increased. Thus, the bandwidth of the proposed MWP phase shifter can be broadened.

IV. CONCLUSION

We have proposed and experimentally demonstrated a continuously tunable MWP phase shifter based on the add-drop type InP/InGaAsP-based MRR. By tuning the optical gain in the MRR, the extinction ratio of the magnitude response at a resonance was decreased to nearly zero, while the large phase shift range was maintained almost unchanged. This unique feature of the MRR is preferable for the implementation of a microwave phase shifter. The proposed phase shifter was experimentally demonstrated. A continuously tunable microwave phase shift over a phase tuning range of 291° from 5 GHz to 20 GHz by tuning the injection current to the PM was implemented. The microwave power variation was controlled as low as 5 dB. The proposed MWP phase shifter is simple and can be expected to be fully integrated on a chip by incorporating the laser source and the PM in the chip. It has great potential for using on integrated system and practical microwave applications.

REFERENCES

- [1] P. Heli, F. Largesse, F. Scotti, G. Serafino, A. Capri, S. Pinna, D. Noori, C. Pori, M. Scaffidi, A. Malacarne, V. Verses, E. Lazzeri, F. Berizzi, and A. Bogoni, "A fully photonics-based coherent radar system," *Nature*, vol. 507, no. 7492, pp. 341-345, Mar. 2014.
- [2] M. H. Alsharif and R. Nordin, "Evolution towards fifth generation (5G) wireless networks: Current trends and challenges in the deployment of millimetre wave, massive MIMO, and small cells," *Telecommun. Syst.*, vol. 64, no. 4, pp. 617-637, Apr. 2017.
- [3] M. Agiwal, A. Roy, and N. Saxena, "Next Generation 5G Wireless Networks: A Comprehensive Survey," *IEEE Commun. Surveys Tuts.*, vol. 18, no. 3, pp. 1617-1655, Feb. 2016.
- [4] J. Yao, "Microwave Photonics," *J. Lightwave Technol.*, vol. 27, no. 3, pp. 314-335, Feb. 2009.
- [5] J. Capmany and D. Novak, "Microwave photonics combines two worlds," *Nature Photon.*, vol. 1, no. 6, pp. 319-330, Jun. 2007.
- [6] R. A. Minasian, E. H. W. Chan, and X. Yi, "Microwave photonic signal processing," *Opt. Express*, vol. 21, no. 19, pp. 22918-22936, Sep. 2013.
- [7] L. R. Chen, "Silicon Photonics for Microwave Photonics Applications," *J. Lightwave Technol.*, vol. 35, no. 4, pp. 824-835, Feb. 2017.
- [8] X. Yi, S. Chew, S. Song, L. Nguyen, and R. Minasian, "Integrated Microwave Photonics for Wideband Signal Processing," *Photonics*, vol. 4, no. 4, pp. 46, Nov. 2017.
- [9] W. Zhang and J. Yao, "Silicon-Based Integrated Microwave Photonics," *IEEE J. Quantum Elect.*, vol. 52, no. 1, pp. 0600412, Jun. 2016.
- [10] Q. Xu, B. Schmidt, S. Pradhan, and M. Lipson, "Micrometre-scale silicon electro-optic modulator," *Nature*, vol. 435, no. 7040, pp. 325-327, May 2005.
- [11] W. Liu, M. Li, R. S. Guzzon, E. J. Norberg, J. S. Parker, M. Lu, L. A. Coldren and J. Yao, "A fully reconfigurable photonic integrated signal processor," *Nature Photon.*, vol. 10, no. 3, pp. 190-195, Feb. 2016.
- [12] J. Capmany, D. Domenech, and P. Munoz, "Silicon graphene waveguide tunable broadband microwave photonics phase shifter," *Opt. Express*, vol. 22, no. 7, pp. 8094-8100, Apr. 2014.
- [13] M. Pu, L. Liu, W. Xue, Y. Ding, L. H. Frandsen, H. Ou, K. Yvind, and J. M. Hvam, "Widely tunable microwave phase shifter based on silicon-on-insulator dual-microring resonator," *Opt. Express*, vol. 18, no. 6, pp. 6172-6182, Mar. 2010.
- [14] X. Liu, C. Sun, B. Xiong, J. Wang, L. Wang, Y. Han, Z. Hao, H. Li, Y. Luo, J. Yan, T. Wei, Y. Zhang, and J. Wang, "Broadband tunable microwave photonic phase shifter with low RF power variation in a high-Q AlN microring," *Opt. Lett.*, vol. 41, no. 15, pp. 3599-3602, Aug. 2016.
- [15] M. Burla, D. Marpaung, L. Zhuang, C. Roeloffzen, M. R. Khan, A. Leinse, M. Hoekman, and R. Heideman, "On-chip CMOS compatible reconfigurable optical delay line with separate carrier tuning for microwave photonic signal processing," *Opt. Express*, vol. 19, no. 15, pp. 21475-21484, Aug. 2011.
- [16] D. G. Rabus, "Integrated Ring Resonators: The Compendium" *Springer Series in Optical Sciences*, no. 4, 2007.
- [17] W. Li, W. Wang, L. Wang, and N. Zhu, "Optical vector network analyzer based on single-sideband modulation and segmental measurement," *IEEE Photon. J.*, vol. 6, no. 2, pp. 1-8, Apr. 2014.
- [18] N. Ehteshami, W. Zhang, and J. Yao, "Optically tunable full 360° microwave photonic phase shifter using three cascaded silicon-on-insulator microring resonators," *Opt. Commun.*, vol. 373, pp. 53-58, Aug. 2016.